J Musculoskelet Neuronal Interact 2019; 19(2):234-244

Journal of Musculoskeletal and Neuronal Interactions JMNI

Original Article

Mitchell's osteotomy augmented with bio-absorbable pins for the treatment of hallux valgus: A comparative finite element study

Emmanouil V. Brilakis[1], Evaggelos Kaselouris[2], Konstantinos Markatos[3], Dimitrios Mastrokalos[4], Christopher Provatidis[5], Nicolas Efstathopoulos[6], Efstathios Chronopoulos[6]

[1]3rd Orthopaedic Department of "Hygeia" General Hospital, Athens, Greece; [2]Technological Educational Institute of Crete Iraklion, Greece; [3]Academy of Athens, Biomedical Research Foundation Athens, Greece; [4]1st Orthopaedic Department of National and Kapodistrian University of Athens, Athens, Greece; [5]Mechanical Design & Control Systems Section National Technical University of Athens, Athens, Greece; [6]2nd Orthopaedic Department of National and Kapodistrian University of Athens, Athens, Greece

Abstract

Background: There is an inadequacy of conventional means to assess the surgical outcomes of a bunion surgery. We used the Finite Element Analysis for evaluating the typical Mitchell's procedure outcomes with or without bio-absorbable pins. **Methods:** We developed a 3D FE model based on the CT images of a female volunteer with hallux valgus. A typical procedure was simulated on the foot model and two pins were virtually inserted for enhancing the fixation. We validated our model by comparing the predicted pressure results with the plantar pressure measured by a specific platform. **Results:** The comparison of the plantar pressure distribution revealed similar patterns. A greater displacement was observed on the medial side of the osteotomy, but it was decreased after using pins. The maximum average pressure under the 1st metatarsal head was decreased after the osteotomy. The respective pressure under the 3rd and 5th metatarsal head was decreased more after using pins, while, under the 2nd and 4th metatarsal head, an increase was developed. **Conclusion:** The use of pins had no significant influence on the healing process but gave additional stability inside the osteotomy and could be used in cases where enhancement is needed. The surgeon should be familiar with the expected stress rising to the other metatarsal, considering the concomitant pathology or the additional interventions that should be performed.

Keywords: Bio-absorbable Pins, Mitchell's Osteotomy, Finite Elements Analysis, Hallux Valgus, Biomechanics

Introduction

The hallux valgus deformity is a common condition that affects individuals of all ages. This condition can lead to painful motion and difficulty wearing footwear. The treatment of hallux valgus has been a topic often studied in the last century, at least. The term hallux valgus defines a subluxation of the first metatarsophalangeal (MTP) joint characterised by lateral deviation and/or rotation of the great toe, and medial deviation of the first metatarsal, which is combined with a prominence, with or without medial soft-tissue enlargement of the first metatarsal head[1,2]. It is not a single, but rather a complex first ray deformity, which is associated with abnormal foot mechanics and is often accompanied by deformities and symptoms in lesser toes[3,4].

More than 150 different surgical techniques have been described and introduced for this deformity's treatment. Although it is considered an entity best treated surgically by orthopaedic surgeons, many times patients prefer using orthotic devices and modified footwear due to fear of surgical complications, deformity relapse, long rehabilitation periods and low patient satisfaction rates monitored with all the surgical techniques', which results in several specific cases[2,5-8]. Surgeons widely believe in the inadequacy of conventional means of assessment of surgical outcomes in the case of bunion surgery[9,10].

Reverdin first described the correction of this deformity

The authors have no conflict of interest.

Corresponding author: Emmanouil Brilakis, 30A Str. Aiolou, 17561 Palaio Faliro, Greece
E-mail: emmanuel.brilakis@gmail.com

Edited by: G. Lyritis
Accepted 29 January 2019

by means of a distal osteotomy of the first metatarsal in 1881[11]. However, it was Mitchell who popularised the bi-planar metaphyseal osteotomy[12,13]. The double step-cut osteotomy through the first metatarsal's neck, is known as the Mitchell's procedure. It was described by Hawkins et al. in 1945 and since then, many changes and modifications have been proposed[14]. Between these procedures, the use of bio-absorbable materials has been studied and published[15-20].

Therefore, it is mandatory for a technique that assesses the load distribution post-surgery for bunion in a foot to understand the change in the foot's loading surfaces after surgery. Recently, a widely-used method that assesses the changes in weight bearing after bunion surgery is the finite elements (FE) analysis[21-25]. We used this method to assess the outcomes of bunion surgery with the technique alone or augmented using one and two bio-absorbable pins for the osteotomy stabilisation.

The FE analysis can measure each component's load distribution and displacement and the internal stresses and strains[26]. Furthermore, this method can analyse the three-dimensional (3D) motion of the bone and the soft tissue deformation under specific conditions[27]. Several 3D FE foot models have been developed to study the biomechanical effects of various normal and pathological conditions[28].

Our study's objective was to assess the use of bio-absorbable pins for augmenting the Mitchell's procedure. We evaluated the biomechanical parameters, such as stress, strain and displacement that were developed in the osteotomy site. We also tested whether there is accordance between the biomechanical data and the clinical outcome, as published in the literature. Eventually, this study's purpose was to assess the optimal treatment strategy for the surgical management of hallux valgus.

Methods

Finite element model development

A 3D finite element model of the foot was developed by volumetric reconstruction of coronal computed tomography (CT) images obtained from the left foot of a healthy female volunteer (age 30, weight 60 kg, height 168 cm). The CT scan properties had a 0.45-mm resolution and 0.75-mm slice spacing. The dataset was imported into MIMICS version 10 medical image processing software (Materialise, Leuven, Belgium) to segment the CT images and obtain the boundaries of the skeleton and the skin. The mesh-processor of the program MIMICS is used for the discretization, providing local treatment to the high curvature and the sharp sub-domains of the bony and soft tissue structures of the model, thus minimizing the need of adaptive refinement of the mesh. FE analysis software ANSYS version 12.0 pre-processing tool (ANSYS, Inc., Canonsburg, PA) was used to process the meshed boundary surfaces and solid parts for each bone in the foot, ankle and the entire external surface were formed.

Twenty-eight bony segments were modelled: talus, cuboid, calcaneus, navicular, 3 cuneiforms, 5 metatarsals, the 14 components of the phalanges, as well as the distal parts of tibia and fibula[29]. Sesamoids were considered fused with the first metatarsal, making an enlarged first metatarsal head. The surface-to-surface contact capability was used to simulate the frictionless contact relationship between articular surfaces. Moreover, fifty-three plantar and dorsal ligaments, along with plantar fascia, were designed by connecting the corresponding attachment points on the bones[29]. The origin and insertion sites of all ligaments were based on their anatomical location according to an anatomy atlas[29]. All bony and ligamentous structures were embedded in a homogenous soft tissue mass that defined the foot's external surface. Furthermore, a horizontal plate was used to simulate ground support, while a frictional contact interaction was established between the plantar surface of the foot and the ground. The coefficient of friction was equal to 0.6[30].

Link tension-only elements were used to simulate the tensile load bearing ligaments. Based on each ligament's individual shape and size, one or multiple link elements were used for the simulation. Five tension-only link elements were used to simulate the plantar fascia. A total of 210,000 ten-node tetrahedral solid elements were considered for the discretisation of bones, cartilages and soft tissue (Figure 1). A mesh sensitivity analysis was performed to ensure the results' independency from the mesh density and that no further mesh refinement was necessary.

Regarding material properties, apart from the encapsulated soft tissue, all parts were defined as homogeneous, isotropic and linearly elastic. The selection of the Young's modulus and the Poisson's ratio, of the normal bony structures, was made by weighing cortical and trabecular elasticity values (Young modulus 7300 MPa, Poisson ratio 0.3)[31]. Literature mechanical properties of cartilage (Young modulus 1 MPa, Poisson ratio 0.4)[32], ligament (Young modulus 260 MPa, Cross-section 18.4 mm^2)[33] and plantar fascia (Young modulus 350 MPa, Cross-section 290.7 mm^2)[34] were also considered[45]. The ground support was attributed a Young Modulus of 72000 MPa and a Poisson ratio of 0.33. With respect to the soft tissue properties, its nonlinear material behaviour was modelled using an isotropic, nearly incompressible, hyper-elastic polynomial formulation as follows:

$$U = \sum_{i+j=1}^{2} C_{ij} (\bar{I}_1 - 3)^i (\bar{I}_2 - 3)^j + \sum_{i=1}^{2} \frac{1}{D_i} (J_{el} - 1)^{2i}$$

In this formulation, U is the strain energy potential, C_{ij} and D_i are parameters of the material, I_1 and I_2 are the first and second deviatoric strain invariants and J_{el} is the elastic volume ratio. A nonlinear function, obtained from *in vivo* ultrasonic measurements of the heel, described the stress-strain dependence of the plantar soft-tissue and values for coefficients C_{ij} and D_i were taken from[35].

Operation simulation

A typical Mitchell's osteotomy was simulated on the foot model with a distal smaller and a proximal osteotomy of the entire metatarsal width (Figure 2). To consider the

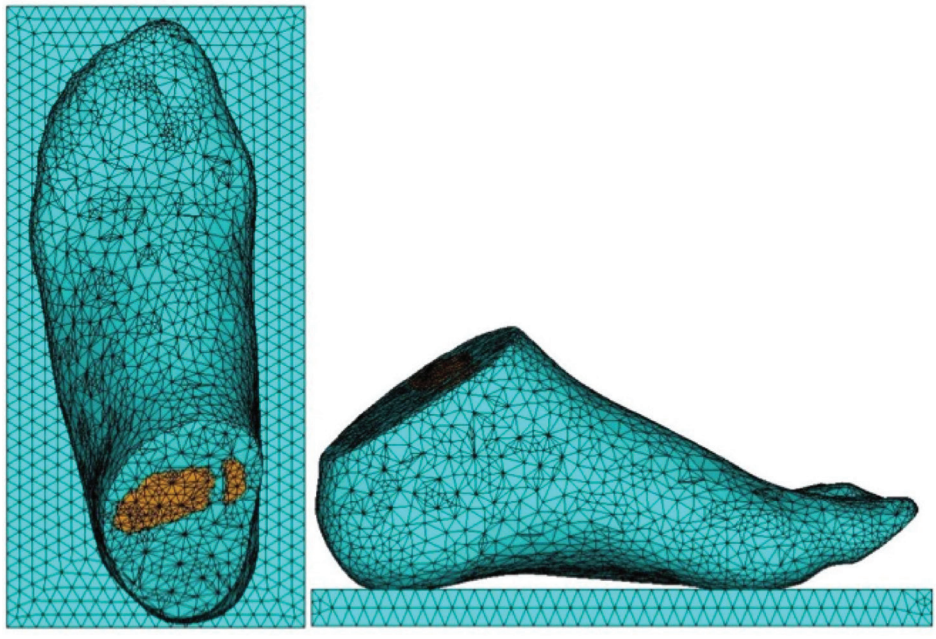

Figure 1. Finite element model consisted of the foot including bones, cartilages, ligaments, and soft tissue. (a) En-face view (b) Profile view.

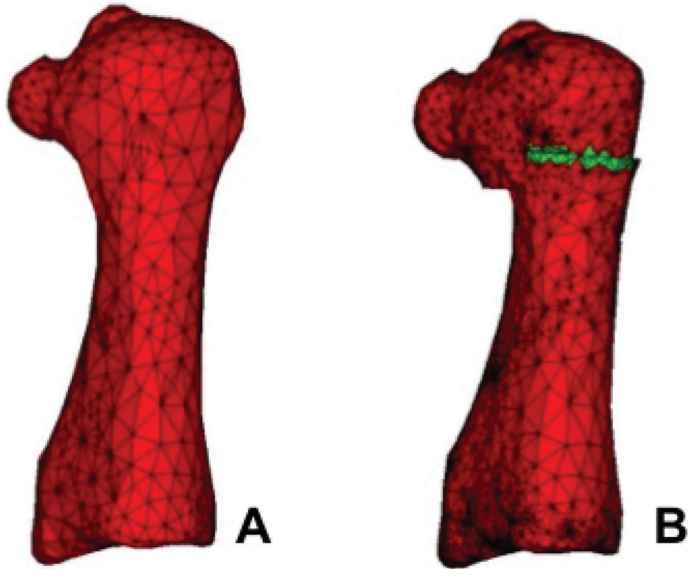

Figure 2. Finite element model of 1st metatarsal bone (a) before and (b) after the simulation of a typical Mitchell's osteotomy.

healing process, and not only the initial and final condition, three different stages were studied, assigning different mechanical properties to the corresponding elements within the osteotomy[45] (Table 1). The first stage represented the initial connective tissue formation, the second stage was the soft callus formation of immature (woven) bone and the third stage was the stiff mature bone formation. The time between the surgery and each one of these stages has not been considered because temporal evolution investigation was not the current study's objective. Two holes, one in the distal and the other in the proximal fragment, were drilled and suture properties were given at the respective elements

Table 1. Mechanical properties attributed to the material within the site of the osteotomy for different stages of healing process.

	Initiative Connective tissue	Immature bone (Soft callus)	Mature bone (Stiff callus)	Normal bone
Young's modulus [MPa]	2	1000	6000	7300
Poisson's ratio (v)	0,167	0,3	0,3	0,3

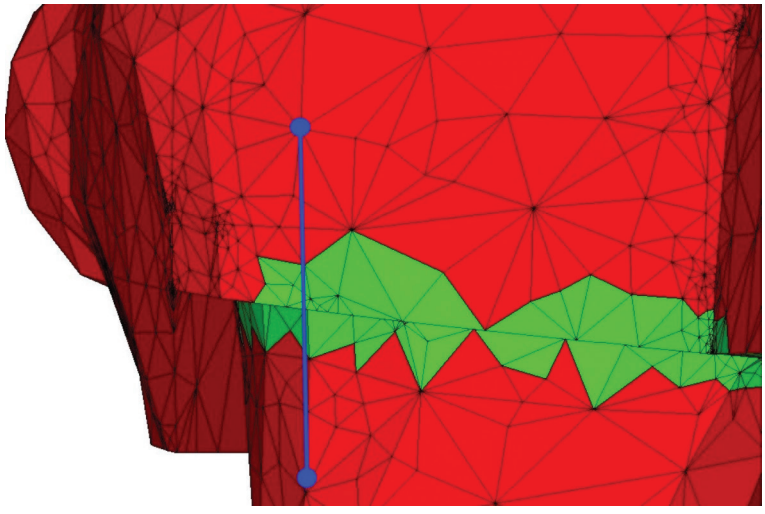

Figure 3. Two holes, one in the distal and the other in the proximal fragment, were drilled and suture properties were given at the respective elements to simulate the fixation method of the step-cut osteotomy.

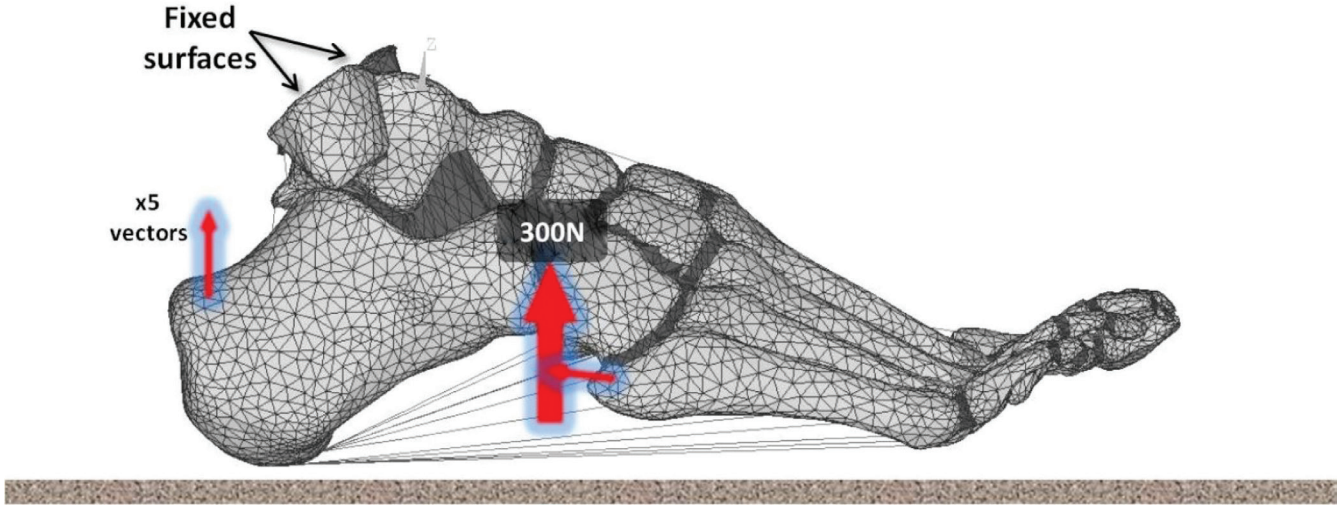

Figure 4. 3D free-body diagram depicting the boundary and loading conditions of the FE model.

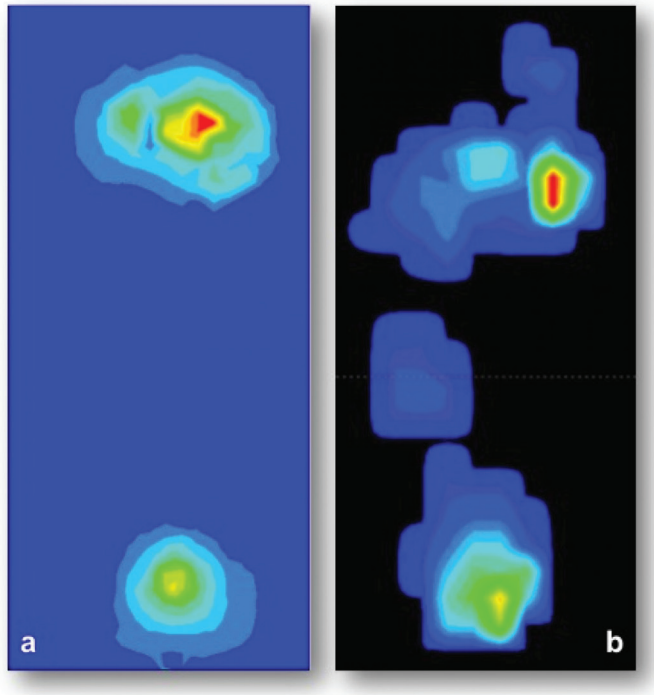

Figure 5. (a) Finite element predicted plantar pressure distribution (MPa), and (b) plantar pressure distribution (MPa) measured with EPS Platform, both for standing in the weight-bearing upright position.

to simulate the fixation method of the step-cut osteotomy (Figure 3). The suture was considered as a biodegradable polymeric biomaterial (Polyglactin 910, glycolide per lactide=9/1) with a Young's modulus of 8.6 GPa[36] and cross-section 0.196 mm^2. Link tension-only element was used to simulate the tensile load bearing suture. Tension changes to the external and of the internal elements were addressed to simulate the soft tissue release during the procedure and the capsuloraphy at the end of the procedure with criterion of the hallux valgus correction. Two pins, that were modeled with their real geometry, were virtually inserted for enhancing the osteotomy fixation. This study used OTPSTM pins with a stiffness of 44 N/mm, length of 20 mm and radius of 1 mm.

Loading conditions

The constraints effects from proximal tissues were simulated by fixing the model's proximal portion. Normal weight bearing and normal gait were evaluated. The applied force vectors to the foot were: the ground reaction force that corresponds to half the body weight (300 N) and the Achilles tendon reaction. The net ground force vector during normal weight bearing was applied perpendicularly to the ground. Ground reaction force was applied to the supporting plate's underside at the centre of the applied pressure on the plantar surface of the foot. The applied pressure was determined from foot pressure analysis measurements. Furthermore, the ground force application point was constrained to allow movement only vertically.

A force of 150 N was applied, based on the assumption that the Achilles tendon force is approximately 50% of the applied force to the foot during balanced standing[37]. This force is defined by 5 equivalent force vectors, and is applied at the posterior extreme of the calcaneus[38]. A 3D free-body diagram illustrates the loading and boundary conditions (Figure 4).

Four 3D finite element models were created in ANSYS, one concerning the pre-operative foot and three concerning an operated foot with a Mitchell's osteotomy of the first metatarsal bone. The 3 models differed in the number of bio-absorbable pins used for augmenting the typical surgical procedure (0, 1 and 2 respectively). A parametric analysis, comparing the 4 different models developed, was carried out in ANSYS to determine the different surgical operations effects (only with suture, with suture and 1 pin and with suture and 2 pins). The effects of the different stabilisation of the same surgical procedure on the first and other metatarsals' ligaments and the effects of using pins on the bones and the developed strains were evaluated. The average displacements within the osteotomy were also examined.

The average peak principal strain of the osteotomy site was recorded, excluding the region of holes due to the pins. The clinical significance of the peak principal strain that is developed during the healing process has been described by Frost[39]. According to his studies, bone remodelling is promoted when the developed strain fluctuates between 50

Table 2. Model Validation. Site-to-site comparison in 6 regions of interest between the measured plantar pressure distribution with the EPS Platform and the FE-computed plantar pressure distribution.

Region Of Interest	Measured (A) Plantar Pressure Distribution (Mpa)	FE-Computed (B) Plantar Pressure Distribution (Mpa)	Difference ([B-A]/B X 100%)
First metatarsal head	0.136	0.143	4,9%
Second metatarsal head	0.055	0.058	5,2%
Third metatarsal head	0.039	0.042	7,1%
Fourth metatarsal head	0.038	0.042	9,5%
Fifth metatarsal head	0.026	0.028	7,1%
Calcaneus	0.112	0.120	6,7%

and 3000 mstrain. Strain values outside this zone do not promote fracture healing.

Foot plantar pressure measurement

Our model's accuracy was secured by comparing the FE-predicted pressure distribution on the plantar surface of the foot to the corresponding distribution from the EPS Platform (LorAn Engineering, Bologna, Italy) (Figure 5). A foot pressure analysis was conducted on the same healthy female volunteer. The volunteer stood upright and barefoot on the platform, and the pressure between the ground and the plantar surface of the foot was measured. Specific software (Footchecker version 4.0; LorAn Engineering) recorded the plantar pressure distribution, peak plantar pressure and centre of pressure. Six clinically significant regions of interest on the plantar surface of the foot were selected to compare the FE-model computed and the foot-scanning measured results. These are the 5 metatarsal heads (#1 to #5) and calcaneal tuberosity (#6).

Results

Validity of the FE model

The measured plantar pressure distribution using the EPS Platform, with the volunteer standing upright in weight bearing, compared to the FE-model predicted distribution revealed similar patterns (Figure 5). The maximum plantar pressure was recorded under the 1st metatarsal head, whether it was predicted by the FE model (0.143 MPa) or measured by the foot scan analysis (0.136 MPa). In the calcaneal region, the maximum plantar pressure, measured by the plantar scan, was 0.112 MPa and 0.120 MPa predicted by the FE model. A detailed comparison of the regions of interest (Table 2) revealed that the maximum deviation (9.5%) between the FE-computed values and experimental data was located under the fourth metatarsal head. The best match (difference: 4.9%) was displayed on the plantar surface of the first metatarsal head. The numerical predicted that plantar pressure was higher in all 6 selected regions of interest, at an average difference of 6.8%, compared to measurements.

Peak principal strain

During the initial healing stage, when connective tissue had been interposed within the osteotomy, the peak principal strain was 5100 mstrain, decreasing at 380 mstrain when a soft callus had been formed (second healing stage). The value of the strain was further decreased to 150 mstrain at the third healing phase of mature bone formation. When one pin was added, the peak principal strain was 4900 mstrain, 240 mstrain, and 140 mstrain, respectively. When two pins were inserted, the respective values were 4000 mstrain, 230 mstrain, and 140 mstrain, respectively (Figure 6).

Stability of the osteotomy

The stability of the osteotomy was examined by the distal displacement in relation to the proximal part. Two neighboured nodes of the plantar, dorsal and medial side were selected and the displacement between them was predicted for each one of the 3 post-operative models (Figure 7). The results are depicted in Table 3. The greater displacement was observed on the medial side in all the 3 models, but it was decreased by 7.5% when using one pin and by 14% when using two. On the dorsal side of the osteotomy the displacement was decreased by 5% when using one pin and by 33% when using two, while the displacement on the plantar side was not influenced by using pins. Due to the pattern of the osteotomy (step cut), we didn't consider the displacement on the lateral side.

Average max stress on the plantar side of the metatarsal heads

The average maximum load on the plantar side of every metatarsal head is depicted in Table 4. For calculating the average maximum value, the ten maximum values of every metatarsal head elements were used. The maximum average pressure under the 1st metatarsal head was decreased after the osteotomy with minimum changes, either with the use of pins or not. The respective pressure under the 3rd and the 5th metatarsal head was decreased after the procedure and decreased further after using pins. Under the 2nd metatarsal head, a significant increase was developed after performing Mitchell's osteotomy. Finally, the pressure under the 4th metatarsal head was increased after the osteotomy and stayed at the same levels after using pins.

Table 3. The displacement within osteotomy measured as the distance of two neighboured nodes during weight bearing postoperatively.

Region of Interest	Post-Operative Displacement Within Osteotomy (μm)		
	1st Model Standard Mitchell's Osteotomy (Stabilization With Suture)	2nd Model Standard Mitchell's Osteotomy Augmented By 1 Pin	3rd Model Standard Mitchell's Osteotomy Augmented By 2 Pins
Dorsal side of the osteotomy	0.64	0.61	0.43
Plantar side of the osteotomy	0.50	0.50	0.50
Medial side of the osteotomy	0.80	0.74	0.69

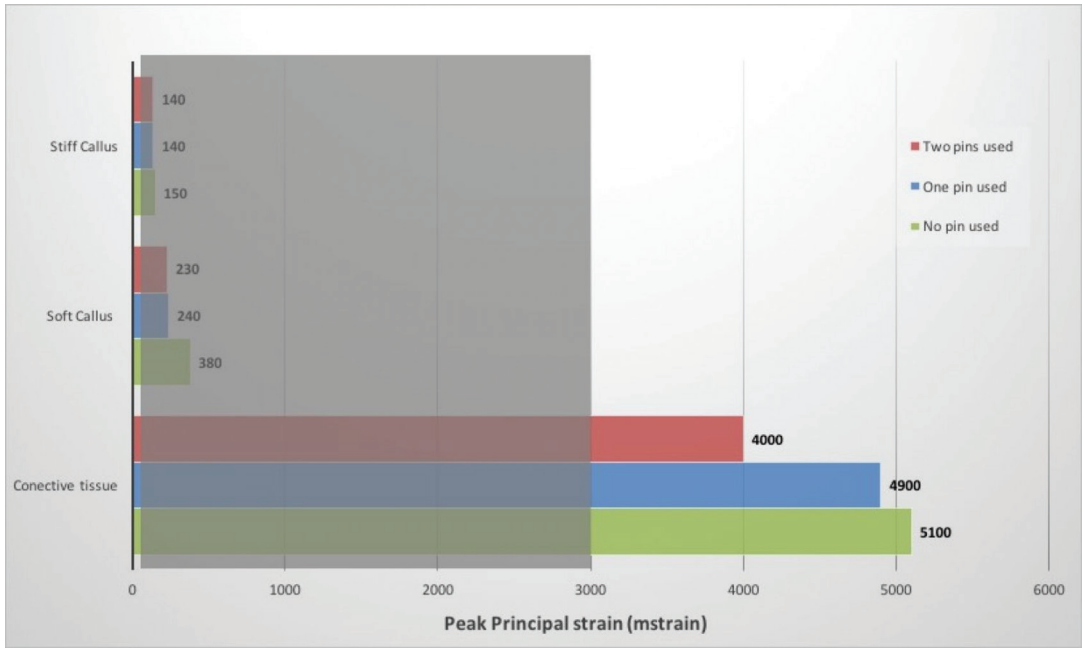

Figure 6. Average peak principal strain within the osteotomy site (excluding the region of holes due to the pins) during the healing process for 3 different models (only with suture, with suture and 1 pin, and with suture and 2 pins). The highlighted area depicts the bone remodelling threshold[39].

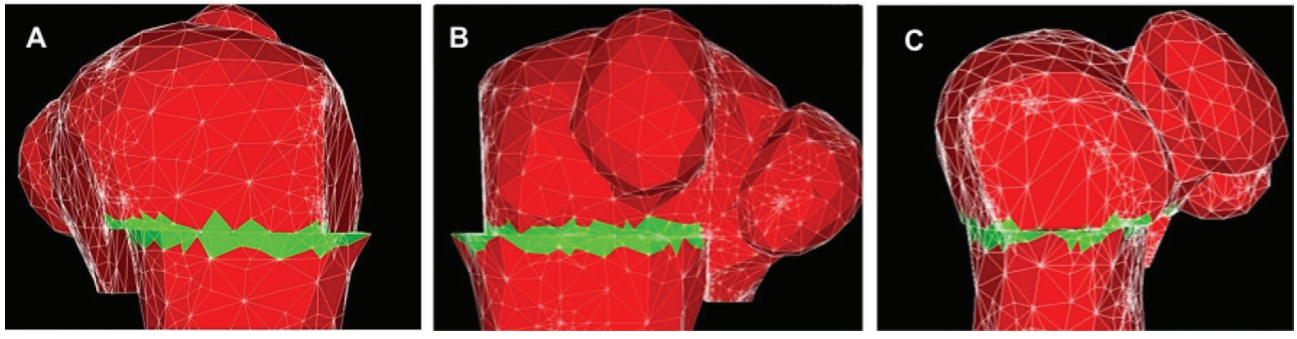

Figure 7. The stability of the osteotomy was examined by the distal displacement in relation to the proximal part. Two neighboured nodes of the dorsal (A) of the plantar (B) and of the lateral (C) side were selected and the displacement between them was predicted for each one of the 3 post-operative models.

Table 4. The average maximum load on the plantar side of every metatarsal head. For calculating the average maximum value, the ten maximum values of every metatarsal head elements were used. Model 1: Foot with HV. Model 2: Correction of HV with Mitchel osteotomy, stabilized with Nylon suture. Model 3: Correction of HV with Mitchel osteotomy, stabilized with Nylon suture and with one bio-absorbable pin. Model 4: Correction of HV with Mitchel osteotomy, stabilized with Nylon suture and with two bio-absorbable pins.

Region Of Interest	Average Max Von Misses stress (MPa)			
	Model 1	Model 2	Model 3	Model 4
First metatarsal head	15.6	15.0	15.3	15.4
Second metatarsal head	8.5	11.1	11.1	11.5
Third metatarsal head	8.8	7.2	6.9	6.8
Fourth metatarsal head	6.0	6.2	6.2	6.1
Fifth metatarsal head	9.6	9.1	8.7	8.6

Table 5. Von Misses stresses developed on the soft tissues which are inserted on the 1st metatarsal bone.

Tissue	Developed stress (A) preoperatively (MPa)	Developed stress (B) postoperatively (MPa)	Difference (B-A)/B x 100%
Dorsal 1st metatarsal ligament	16.5	16.8	2%
Dorsal ligament with 2nd metatarsal bone	1.6	5	68%
Deep transverse ligament with 2nd metatarsal bone	0.6	2.2	73%
Metatarsophalangeal joint capsule	1.8	4.2	57%
Adductor hallucis muscle	1.7	1.7	-
Plantar aponeurosis	0.7	0.7	-

Stress on the soft tissues inserted on the 1st metatarsal bone

The average von Mises stress developed pre-operatively on the foot suffering from HV and post-operatively, after the correction with Mitchell's osteotomy, stabilised with a Nylon suture is depicted in Table 5. The dorsal 1st metatarsal ligament developed the maximum stress with 16.5 MPa, which was increased by 2% post-operation. The stress on the dorsal ligament with the 2nd metatarsal bone was increased by 68% (from 1.6 to 5 MPa) after the operation and on the deep transverse ligament with the 2nd metatarsal bone by 73% (from 0.6 to 2.2 MPa). The joint capsule developed 57% more stress post-operatively (from 1.8 to 4.2 MPa), while the adductor hallucis muscle and the plantar fascia developed the same stress pre- and post-operatively.

Discussion

Since the 1980s, bio-absorbable materials have been increasingly used in orthopaedic surgery, mainly for fracture management as fixation devices, with satisfactory outcomes[40]. Moreover, their use can be expanded for fixation after osteotomies without allowing full weight bearing during the early post-operative period[41]. One main advantage of such devices is that their removal doesn't require a second procedure[42]. The main reported disadvantage is the possible early host immune reaction, which leads to the destruction and aseptic inflammation of the surgical site[43]. However, the use of bio-absorbable materials is not connected with bacterial infection and are generally considered safe[44].

Using bio-absorbable pins for a hallux valgus surgery relates to a rational fixation for greater osteotomy stability compared to that of a suture-only stabilised osteotomy. Nevertheless, their use has not been established as the gold standard until now. Additionally, the rigid fixation has raised questions concerning the way they may affect the 1st metatarsal bone's ligaments and the stress, which is transferred on the neighbouring bones, as far as anatomic and weight-bearing conditions are concerned[19].

Using a finite element analysis is considered as a sound method and has been used for evaluating a body part's 3D model to explore the deviation from a normal anatomy and stress model in the components attached. Therefore, its use is justified to investigate the stress applied and to compare models for deviations from a normal condition. Additionally, it is a powerful and sensitive tool, which can be used to compare surgery outcomes for anatomy alterations and stress application in various bone and ligament sites[15-27,45].

This study's first outcome is that additionally using pins has no any significant positive or negative influence on the healing process. Moreover, additionally using pins (one or two) does not change the need for an initial small period of non, or partial weight bearing using special footwear. Calculating this period would be very interesting, but our model is not capable of this. However, using additional pins may increase the fixation's stability, thereby decreasing the displacement measured inside the osteotomy. Clinically applying this information could be useful in cases where the surgeon is doubtful or not satisfied enough concerning the stability of the procedure. This is an option that intra-operatively can give him the chance to enhance the stability of the osteotomy by augmenting the suture fixation with one or two pins.

In our study, we also observe that in the case of the osteotomised 1st metatarsal bone with the Mitchell's modified technique, maximum stresses in the 3rd and 5th metatarsal bones are decreased compared to normal. Considering that the ligaments are the main transport mean of the stress to the 2nd and other metatarsals, greater stresses are developed due to ligaments strain and these differences are compensated in the other metatarsal bones and joints. Thus, it is obvious that a change in anatomy and stresses compresses or decompresses the other metatarsals. Moreover, in the case of the model with hallux valgus, maximum stress is applied on the 5th metatarsal bone (excluding the 1st metatarsal), whereas in the osteotomised model, maximum stress is applied on the 2nd metatarsal bone (excluding the 1st metatarsal).

Thus, depending the concomitant pathologies, the surgeon can use or avoid the additional pins for adjusting the pressure under the metatarsal heads. This can significantly improve the outcome and immediate post-operative weight-bearing stage of the foot, as far as correcting hammer toe, claw toe or bunionette deformities are concerned. For example, transferring maximum stress on the 2nd metatarsal can help in case of a simultaneously-performed osteotomy of the 3rd metatarsal to correct deformities in those bones (e.g. with Helal or Weil osteotomies). In such cases, which are relatively common, using pins and subsequently transferring the load is useful in the weight bearing protection of the 3rd osteotomised metatarsal. Moreover, such a decompression rationale can be quite useful in cases where tenotomies are performed on the extensor tendons to correct mild deformities of the 3rd toe. In the case of the 5th metatarsal, additional decompression can reduce the stress in the case of a simultaneous bunionette deformity correction.

However, the present study has some limitations. The operation was virtually simulated on the developed model with hallux valgus based on the orthopedic surgeon knowledge and experience. This method was selected, because modelling based on the post-operative CT images have some difficulties due to the trauma and its wrapping (tight bandages), the artifacts from the metallic stiches and the use of external splint and the soft tissue edema. This study had not considered the capsule suturing and soft tissue repair post-surgery due to the practical difficulty in modelling the above conditions. The developed models were static and the centre of pressure was assumed to be unchanging. However, it has a dynamic change during standing or walking. Moreover, only standing and balanced loads were simulated. However, the loads are not always balanced during bearing. Furthermore, only the forces of the Achilles tendon and peroneus muscles were simulated, but not of other intrinsic and extrinsic muscles. The movement of the distal tibiofibular syndesmosis was not considered because the surfaces over the talus were fixed. Incorporating every soft tissue structure (skin layers, fat pad, intrinsic and extrinsic muscles, the ankle joint, and the distal parts of tibia and fibula) is needed to design a more precise model. However, analysing such a detailed model requires a lot of time and a huge amount of computer memory.

Conclusions

Our study of the Mitchell's procedure, augmented with bio-absorbable pins for the management of hallux valgus with the method of finite elements, found that the use of two bio-absorbable pins is more stable and secures the first metatarsal bone osteotomy because the stress is divided between the pins, although not equally, and a deformity is less likely to compromise their structural integrity, deform, translate or even crack them. Additionally, using bio-absorbable pins, compared to sutures for fixating the osteotomy, seems to transfer stress from the 3rd and 5th metatarsal bones to the 2nd one. Thus, it is very useful in cases where osteotomies or tenotomies of the extensor tendons are performed to correct deformities of the respective toes. In these cases, the decompression of these metatarsals could improve healing, securing the osteotomy in the short-term results and reducing the recurrence rate in long-term results.

References

1. Sammarco VJ. Surgical Correction of Moderate and Severe Hallux Valgus. Proximal Metatarsal Osteotomy with Distal Soft-Tissue Correction and Arthrodesis of the Metatarsophalangeal Joint. J Bone Joint Surg Am. 2007;89:2520-2531.
2. Coughlin MJ, Mann RA. Hallux Valgus In: Coughlin MJ, Mann RA, Saltzman CL editors. Surgery of the foot and ankle, 8th Edition, St. Louis: Mosby; 2007. p. 183-362.
3. Haines RW, McDougall A. The anatomy of hallux valgus. J Bone Joint Surg Br 1954;36-B(2):272-93.
4. Brahms MA. Common foot problems. Foot Ankle Int 1995;16(10):594-603.
5. Torkki M, Malmivaara A, Seitsalo S, Hoikka V, Laippala P, Paavolainen P. Surgery vs orthosis vs watchful waiting for hallux valgus: a randomized controlled trial. JAMA 2001;285:2474-2480.
6. Robinson AH, Limbers JP. Modern concepts in the treatment of hallux valgus. J Bone Joint Surg Br 2005; 87:1038-1045.

7. Trnka HJ. Osteotomies for Hallux Valgus Correction. Foot Ankle Clin N Am 2005;10:15-33.
8. Sammarco VJ, Acevedo J. Stability and fixation techniques in first metatarsal osteotomies. Foot Ankle Clin 2001;6:409-32.
9. Mortka K, Lisiński P. Hallux valgus-a case for a physiotherapist or only for a surgeon? Literature review. J Phys Ther Sci 2015;27(10):3303-7.
10. Mann RA. Hallux valgus. Instr Course Lect 1986;35:339-53.
11. Beck EL. Modified Reverdin technique for hallux abductor valgus (with increased proximal articular set angle of the first metatarsophalangeal joint). J Am Podiatry Assoc 1974;64(8):657-66.
12. Chandler LM. First metatarsal head osteotomies for the correction of hallux abductor valgus. Clin Podiatr Med Surg 2014;31(2):221-31.
13. Grannis WR, Meier AW, Tanner JB. Surgical treatment of bunions; distal metatarsal osteotomy. Calif Med 1956; 85(4):245-7.
14. Holmstroem B. Hawkins-Mitchell metatarsal osteotomy in hallux valgus. Nord Med 1964;23;72:900-2.
15. Nikolaou VS, Korres D, Xypnitos F, Lazarettos J, Lallos S, Sapkas G, Efstathopoulos N. Fixation of Mitchell's osteotomy with bio-absorbable pins for treatment of hallux valgus deformity. Int Orthop 2009;33(3):701-6.
16. Alcelik I, Alnaib M, Pollock R, Marsh DJ, Tulloch CJ. Bio-absorbable fixation for Mitchell's bunionectomy osteotomy. J Foot Ankle Surg 2009;48(1):9-14.
17. Porter MD, Anderson MG. Results of bio-absorbable fixation of metatarsal osteotomies. Am J Orthop (Belle Mead NJ) 2004;33(12):609-11.
18. Caminear DS, Pavlovich R Jr, Pietrzak WS. Fixation of the chevron osteotomy with an absorbable copolymer pin for treatment of hallux valgus deformity. J Foot Ankle Surg 2005;44(3):203-10.
19. Gill LH, Martin DF, Coumas JM, Kiebzak GM. Fixation with bio-absorbable pins in chevron bunionectomy. J Bone Joint Surg Am 1997;79(10):1510-8.
20. Winemaker MJ, Amendola A. Comparison of bio-absorbable pins and Kirschner wires in the fixation of chevron osteotomies for hallux valgus. Foot Ankle Int 1996;17(10):623-8.
21. Wai-Chi Wong D, Wang Y, Zhang M, Kam-Lun Leung A. Functional restoration and risk of non-union of the first metatarso-cuneiform arthrodesis for hallux valgus: A finite element approach. J Biomech 2015; 48(12):3142-8.
22. Morales-Orcajo E, Bayod J, Becerro-de-Bengoa-Vallejo R, Losa-Iglesias M, Doblare M. Influence of first proximal phalanx geometry on hallux valgus deformity: a finite element analysis. Med Biol Eng Comput 2015; 53(7):645-53.
23. Wong DW, Zhang M, Yu J, Leung AK. Biomechanics of first ray hypermobility: an investigation on joint force during walking using finite element analysis. Med Eng Phys 2014;36(11):1388-93.
24. Trabelsi N, Milgrom C, Yosibash Z. Patient-specific FE analyses of metatarsal bones with inhomogeneous isotropic material properties. J Mech Behav Biomed Mater 2014;29:177-89.
25. Matzaroglou C, Bougas P, Panagiotopoulos E, Saridis A, Karanikolas M, Kouzoudis D. Ninety-degree chevron osteotomy for correction of hallux valgus deformity: clinical data and finite element analysis. Open Orthop J 2010;4:152-6.
26. Yu J, Cheung JT, Fan Y, Zhang Y, Leung AK, Zhang M. Development of a finite element model of female foot for high-heeled shoe design. Clin Biomech (Bristol, Avon) 2008;23(Suppl.1):S31-8.
27. Budhabhatti SP, Erdemir A, Petre M, Sferra J, Donley B, Cavanagh PR. Finite element modeling of the first ray of the foot: a tool for the design of interventions. J Biomech Eng 2007;129(5):750-6.
28. Kai T, Cheng-Tao W, Dong-Mei W, Xu W. Primary analysis of the first ray using a 3-dimension finite element foot model. Conf Proc IEEE Eng Med Biol Soc 2005;3:2946-9.
29. Schuenke M, Schulte E, Schumacher U. General Anatomy and the Musculoskeletal System (THIEME Atlas of Anatomy), ed 1, Stuttgart: Thieme; 2006.
30. Zhang M, Mak AFT. *In vivo* friction properties of human skin. Prosthet Orthot Int 1999;23:135-141.
31. Gefen A, Megido-Ravid M, Itzchak Y, Arcan M. Biomechanical analysis of the three-dimensional foot structure during gait: a basic tool for clinical applications. J Biomech Eng 2000;122:630-639.
32. Athanasiou KA, Liu GT, Lavery LA, Lanctot DR, Schenck RC. Biomechanical topography of human articular cartilage in the first metatarsophalangeal joint. Clin Orthop Relat Res 1998;348:269-281.
33. Siegler S, Block J, Schneck CD. The mechanical characteristics of the collateral ligaments of the human ankle joint. Foot Ankle 1988;8:234-242.
34. Wright D, Rennels D. A study of the elastic properties of plantar fascia. J Bone Joint Surg Am 1964;46:482-492.
35. Lemmon D, Shiang TY, Hashmi A, Ulbrecht JS, Cavanagh PR. The effect of insoles in therapeutic footwear: a finite element approach. J Biomech 1997;30:615-620.
36. Chih-Chang Chu. Biodegradable Polymeric Biomaterials: An Updated Overview. In: Bronzino JD, editor. The Biomedical Engineering Handbook: Second Edition. Boca Raton: CRC Press LLC; 2000. chapter 41, p. 1-22.
37. Simkin A. Structural analysis of the human foot in standing posture. Ph.D. Thesis, Tel Aviv University, Tel Aviv, Israel; 1982.
38. Cheung JT, Zhang M, An KN. Effects of plantar fascia stiffness on the biomechanical responses of the ankle-foot complex. Clin Biomech 2004;19:839-846.
39. Frost HM. The biology of fracture healing. An overview for clinicians. Part I. Clin Orthop Relat Res 1989; 248:283-293.
40. Kontakis GM, Pagkalos JE, Tosounidis TI, Melissas J,

Katonis P. Bio-absorbable materials in orthopaedics. Acta Orthop Belg 2007;73(2):159-69.
41. Ciccone WJ 2nd, Motz C, Bentley C, Tasto JP. Bio-absorbable implants in orthopaedics: new developments and clinical applications. J Am Acad Orthop Surg 2001;9(5):280-8.
42. Rokkanen PU. Bio-absorbable fixation devices in Orthopaedics and Traumatology. Ann Chir Gynaecol 1998;87(1):13-20.
43. Santavirta S, Takagi M, Gómez-Barrena E, Nevalainen J, Lassus J, Salo J, Konttinen YT. Studies of host response to orthopedic implants and biomaterials. J Long Term Eff Med Implants 1999;9(1-2):67-76.
44. Parks RM, Nelson G. Complications with the use of bio-absorbable pins in the foot. J Foot Ankle Surg 1993;32(2):153-61.
45. Brilakis E, Kaselouris E, Xypnitos F, Provatidis CG, Efstathopoulos N. Effects of foot posture on fifth metatarsal fracture healing: a finite element study. J Foot Ankle Surg 2012;51(6):720-8.